Probability Analysis of Bistable Composite Laminates using the Subset Simulation Method

Saeid Saberi[1], Azam Abdollahi[2], Michael I Friswell[3*]

[1]Department of Mechanical Engineering, Isfahan University of Technology, Isfahan 84156-83111, Iran.
[2]Department of Civil Engineering, University of Sistan and Baluchestan, Zahedan 98155−987, Iran.
[3]College of Engineering, Swansea University, Bay Campus, Swansea SA1 8EN, United Kingdom.
*m.i.friswell@swansea.ac.uk

Abstract

Bistable composite laminates are advanced composite structures which are potential candidates for morphing structure applications. The geometrical dimensions, material properties, ambient temperature and moisture have significant effects on the bistable behaviour, and the effect of uncertain parameters should be quantified. Reliability analysis is well established for the quantitative assessment of the probability of an event due to parameter uncertainty. Thus, subset simulation is applied to the reliability and sensitivity analysis of bistable composite plates with multiple random parameters. The bistability probability is estimated using the principle of minimum energy; the Rayleigh-Ritz method is used to develop the equations of motion and the limit state function. The results indicate that the stacking sequence has a large effect on bistability probability, and cross-ply composite laminates are most likely to be bistable. Moreover, moisture absorption by the laminate can dramatically reduce this probability. The sensitivity reliability analysis demonstrates that for bistable laminates subject to humidity, the coefficient of thermal and moisture expansions have the greatest influence on the bistability probability. However, for bistable laminates without moisture the thickness is the most important factor. The accuracy and efficiency of the subset simulation method is validated by Monte Carlo simulation.

Keywords: Bistable Composite Laminate, Reliability Analysis, Subset Simulation, Sensitivity Analysis, Uncertainty Quantification, Advanced Composites.

1. Introduction

The specific features of bistable composite laminates, such as the ability to change shape, are increasingly employed in various fields, including aero-structures and surfaces, soft robotics, de-icing system, solar tracking device, and energy harvesting [1–10]. The practical use of these structures requires a range of analyses in order to understand the effects of different factors on their bistability characteristics. Of particular interest is the variety of uncertainties in the composite materials due to the production and manufacturing processes used. This leads to variability in the mechanical properties, which affects the analytical and experimental results, and has a significant influence upon structural responses and reliability [11,12]. Consequently, to improve the performance of composite laminates, these uncertainties should be recognized and analyzed.

Hyer [13] investigated the behavior of an unsymmetrical composite laminate under thermal loads, and found there are two cylindrical stable configurations, which classical lamination theory could not predict. Hyer and Hamamoto [14,15] then presented an analytical nonlinear model to study these structures, which was based on the total potential energy and the Rayleigh-Ritz technique, considering the geometrical nonlinearity. Residual stress created by the manufacturing process leads to a geometrical nonlinearity in these structures so that a small change in the design parameters makes a noticeable variation to their responses. The material properties, fiber ply angles and geometric dimensions have a great impact on the deformation of the stable configurations. A number of researchers have investigated the effect of the plate geometry and lay-up on the bistable behavior. Ren et al. [16] investigated the shape deviations of initially cylindrical composite shells with four different stacking sequences after curing. Betts et al. [17] considered the sensitivity of the displacement of the bistable composite laminate to the additional resin layer, the variation of ply thickness and the ambient temperature for various lay-ups, using an analytical method and a novel technique to map the surface. They noted that $[0 \pm \theta/90 \pm \theta]$ lay-ups of bistable composite laminates in their stable states have opposite and equal curvatures. Giddings et al. [18] investigated the cured shapes of cross-ply and angle-ply bistable composite plates subject to thermal loads by considering an excess resin layer and using finite element and experimental methods. Tawfik et al. [19] examined the bistable characteristics of unsymmetric cross-ply laminates in rectangular, trapezoidal and triangular planforms. Pirrera et al. [20] used a combination of a Ritz model and path-following algorithms to study the effects of important parameters such as temperature variation, panel geometry and lay-up on the stable states of bistable cylindrical panels. Mattioni et al. [21] obtained the stable states of multistable unsymmetric laminates using both finite element analysis and an analytical method. The panels were designed with two square plates using symmetric and unsymmetric stacking sequences, which were analyzed for different thicknesses and lay-ups.

Environmental conditions play a considerably role in the response of these structures. Various researchers have studied the influence of humidity and temperature on the bistable behavior of composite laminates. Moore et al. [22] determined the thermal response of bistable composite plates with several lay-ups using the nonlinear finite element method and illustrated that the thermal expansion coefficient has the highest impact on the stable configurations. Zhang et al. [23] used a digital image processing technique to demonstrate experimentally the bistable characteristic of an anti-symmetric laminated cylindrical shell in different temperature situations. The results showed that as the temperature increases, the snap-through load and curvatures decrease. Zhang et al. [24] examined the bistable behaviour of anti-symmetric composite shells under thermo-mechanical loading when the properties of the composite material are assumed to vary with temperature. The influence of the thermal load, both as a uniform temperature field and as through-thickness thermal gradients, on the stable states of bistable composites were investigated. Fujioka et al. [25] used analytical formulations and finite element simulations to analyze bistable composite rods made of plain woven fabrics. The mechanical properties were considered to be temperature-dependent and the impact of temperature on the deployment behavior was studied. Che et al. [26] studied the cured shapes and the deformation states of fiber metal laminates with different initial curvatures under thermal load. They used analytical, finite element and experimental methods to determine the effect of the side length and the stacking sequence on the stable configurations.

Etches et al. [27] studied hygroscopic effects, and used an experiment to investigate the effects of moisture absorption on the characteristics of bistable composite laminates, such as curvatures, snap-through loads and geometric changes. Moisture absorption was shown to have a significant effect on the geometry, and the chord length increased by more than 50% in relative humidity of 65%. Zhang et al. [28] examined experimentally the hygroscopic effects on the bistable parameters of composite cylindrical shells and showed that snap-through and back loads between two stable states increased with increased moisture. Wu et al. [29] developed an analytical method based on the minimum energy principle to investigate the hydrothermal effect on the bistability of cylindrical shell structures. An increase in the temperature and humidity led to an increase in the principal curvature, and the temperature had the larger influence.

Brampton et al. [30] studied the effect of material properties, environmental conditions and geometrical uncertainties on the major curvature of bistable composite laminates. The sensitivity of the cured shape to each parameter was determined by considering a ±5% change in the parameter using the total potential energy and the Rayleigh-Ritz method. Recently, Saberi et al. [12] investigated the reliability of a cross-ply bistable laminate using the combination of minimum potential energy, Rayleigh-Ritz and Monte Carlo methods. The thickness and coefficient of thermal expansion were shown to have a larger effect on the bistability behavior compared to other input parameters.

Although a large body of research has been performed on various aspects of the static behaviour of bistable composites to improve the performance of these structures, the exact influence of different parameters on their behaviour should be quantified. Therefore, in order to examine the exact effect of each input variable on the bistable behaviour of these structures, this research work studies the reliability and sensitivity analysis of bistable composite laminates.

In this paper, for the first time, a sensitivity analysis with respect to random variables, including material properties, geometry features and environmental conditions, is studied by a combination of the principle of minimum potential energy, the Rayleigh-Ritz and the Subset Simulation (SS) methods by considering the input parameters simultaneously. Sensitivity and uncertainty analysis play a special role in the design of composite structures. The effect of uncertainties in the input parameters on the behavior of structures is investigated using uncertainty analysis, and the sensitivity analysis examines the contribution of the uncertainty in each of input parameters to the uncertainties in the output results. The principle of minimum potential energy and the Rayleigh-Ritz method are used to derive the equations of the bistable composite laminates and the Limit State Function (LSF) is defined in the context of bistability. The examples given in the paper assume that a bistable behavior is not required; a similar formulation for applications that require a bistable structure could define failure as a mono-stable structure. Typical probability distributions for the parameters are then used to estimate the bistability probability for five kinds of bistable composite laminates by Monte Carlo Simulation (MCS) and the SS method. The effect of the uncertain parameters on the structural response of bistable laminates is also studied using a sensitivity analysis, both with and without moisture effects. This work can help in the robust design of complex composite structures.

2. Theoretical Formulation for a Bistable Laminate

The properties of a bistable laminate are formed during the curing process and rely on the nonlinear geometry. Thus the von-Karman strain terms are used to predict the nonlinear behavior and the stable configurations. It should be mentioned that the bistable composite laminates are assumed to be thin, which means the Kirchhoff hypothesis is utilized and the layers are assumed to be in a state of plane stress [15]. The total strains defined as

$$\begin{Bmatrix} \varepsilon_{xx} \\ \varepsilon_{yy} \\ \varepsilon_{xy} \end{Bmatrix} = \begin{Bmatrix} {\varepsilon^0}_{xx} \\ {\varepsilon^0}_{yy} \\ {\varepsilon^0}_{xy} \end{Bmatrix} + z \begin{Bmatrix} {\kappa^0}_{xx} \\ {\kappa^0}_{yy} \\ {\kappa^0}_{xy} \end{Bmatrix} \tag{1}$$

where $(i,j = x,y)$ ${\varepsilon^0}_{ij}$ are the strain vectors at the mid-plane, which are expressed as

$$\begin{bmatrix} {\varepsilon^0}_{xx} \\ {\varepsilon^0}_{yy} \\ {\varepsilon^0}_{xy} \end{bmatrix} = \begin{bmatrix} \frac{\partial U_0}{\partial x} + \frac{1}{2}\left(\frac{\partial W_0}{\partial x}\right)^2 \\ \frac{\partial V_0}{\partial y} + \frac{1}{2}\left(\frac{\partial W_0}{\partial y}\right)^2 \\ \frac{1}{2}\left(\frac{\partial U_0}{\partial y} + \frac{\partial V_0}{\partial x} + \frac{\partial W_0 \partial W_0}{\partial x \ \partial y}\right) \end{bmatrix} \tag{2}$$

In Eq. (1), the curvatures at the mid-plane, ${\kappa^0}_{ij}$, are obtained as

$$\begin{bmatrix} {\kappa^0}_{xx} \\ {\kappa^0}_{yy} \\ {\kappa^0}_{xy} \end{bmatrix} = \begin{bmatrix} -\frac{\partial^2 W_0}{\partial x^2} \\ -\frac{\partial^2 W_0}{\partial y^2} \\ -2\frac{\partial^2 W_0}{\partial x \partial y} \end{bmatrix} \tag{3}$$

In Eqs. (2) and (3), U_0, V_0,W_0 denote the out-of-plane and in-plane displacements in the *x, y* and *z* directions, respectively.

The principle of minimum potential energy is employed to establish the equations of motion. The total potential energy of the composite laminate is

$$\Pi = \int_v \left(\frac{1}{2} \overline{Q}_{ij} \varepsilon_i \varepsilon_j - \overline{Q}_{ij} \alpha_{ij} \varepsilon_i \Delta T - \overline{Q}_{ij} \beta_{ij} \varepsilon_i \Delta M \right) dv \tag{4}$$

where $i,j = (1, 2, 6)$, $\overline{Q}_{ij}$ is the reduced stiffness matrix, α_{ij} are the thermal expansion coefficients, β_{ij} are the moisture coefficients, ΔT is the temperature difference between the cured and ambient temperatures, and ΔM is the difference in moisture saturation.

By using Eqs. (1) and (4) and integrating through the thickness, Eq. (4) gives

$$\Pi = \int_{-L_y/2}^{L_y/2} \int_{-L_x/2}^{L_x/2} \frac{1}{2} \begin{bmatrix} \varepsilon^0 \\ \Delta\kappa \end{bmatrix}^T \begin{bmatrix} A & B \\ B & D \end{bmatrix} \begin{bmatrix} \varepsilon^0 \\ \kappa \end{bmatrix} - \begin{bmatrix} N^t \\ M^t \end{bmatrix}^T \begin{bmatrix} \varepsilon^0 \\ \kappa \end{bmatrix} - \begin{bmatrix} N^m \\ M^m \end{bmatrix}^T \begin{bmatrix} \varepsilon^0 \\ \kappa \end{bmatrix} dxdy \tag{5}$$

where

$$\varepsilon^0 = \left\{ \varepsilon^0{}_{xx} \quad \varepsilon^0{}_{yy} \quad \varepsilon^0{}_{xy} \right\}^T, \qquad \kappa^0 = \left\{ \kappa^0{}_{xx} \quad \kappa^0{}_{yy} \quad \kappa^0{}_{xy} \right\}^T,$$

$$N^{t,m} = \left\{ N^{t,m}{}_x \quad N^{t,m}{}_y \quad N^{t,m}{}_{xy} \right\}^T, \qquad M^{t,m} = \left\{ M^{t,m}{}_x \quad M^{t,m}{}_y \quad M^{t,m}{}_{xy} \right\}^T,$$

L_x and L_y are the dimensions of the plate, and *A*, *B* and *D* are, respectively, the in-plane, coupling and bending stiffness matrices. $N^{t,m}$ and $M^{t,m}$ are the hydrothermal stress and moment resultants, respectively.

The displacement fields are assumed to take the form

$$U_0(x,y) = \sum_{i=1}^{m}\sum_{j=1}^{n} t_{ij} x^i y^{2(j-1)}$$

$$V_0(x,y) = \sum_{i=1}^{m}\sum_{j=1}^{n} s_{ij} x^{2(i-1)} y^j$$

$$W_0(x,y) = \sum_{i=1}^{m}\sum_{j=1}^{n} r_{ij} x^{2(i-1)} y^{2(j-1)} \tag{6}$$

where t_{ij}, s_{ij} and r_{ij} are unknown coefficients. $X = \{t_{ij}, s_{ij}, r_{ij}\}^T$ is the vector of unknown coefficients. In this study, the center of the plate is fixed and the edges are free, and thus the proposed displacement fields satisfy these boundary conditions. Moreover, According to Eqs. (3) and (6) curvatures are considered variable and not constant. It is assumed that the laminate includes perfectly bonded layers and there is no slip between the adjacent layers, which means the displacement components are continuous through the thickness.

By substituting Eq. (6) in Eq. (5) and integrating, the total potential energy is obtained as a function of the coefficients of the displacement fields. The equilibrium states are determined using the principle of minimum potential energy; the variations with respect to the unknown coefficients are obtained and the resulting expressions are set to zero. Thus

$$\Pi = \Pi(r_{ij}, s_{ij}, t_{ij})$$

$$\delta\Pi = \frac{\partial \Pi}{\partial r_{ij}}\delta r_{ij} + \frac{\partial \Pi}{\partial s_{ij}}\delta s_{ij} + \frac{\partial \Pi}{\partial t_{ij}}\delta t_{ij} = 0 \tag{7}$$

This equation can be rewritten as

$$\begin{cases} \dfrac{\partial \Pi}{\partial r_{ij}} = 0 \\ \dfrac{\partial \Pi}{\partial s_{ij}} = 0 \\ \dfrac{\partial \Pi}{\partial t_{ij}} = 0 \end{cases} \tag{8}$$

Equation (8) is a system of nonlinear equations that are solved using the Newton-Raphson method. There are three types of solution of this equation, two of which are stable equilibria and the third is an unstable equilibrium state. To obtain the stable shapes of the laminates and solve the system of equations by the Newton-Raphson method the initial values should be defined in such a way that the curvature in one direction is significantly more (or less) than the curvature in the other direction.

The equilibrium configuration of a plate will stable if the Jacobian matrix of the potential energy is definite positive. The Jacobian may be calculated as

$$J = \begin{bmatrix} \dfrac{\partial^2 \Pi}{\partial {r_{ij}}^2} & \dfrac{\partial^2 \Pi}{\partial r_{ij} \partial t_{ij}} & \dfrac{\partial^2 \Pi}{\partial r_{ij} \partial s_{ij}} \\ \dfrac{\partial^2 \Pi}{\partial t_{ij} \partial r_{ij}} & \dfrac{\partial^2 \Pi}{\partial {t_{ij}}^2} & \dfrac{\partial^2 \Pi}{\partial t_{ij} \partial s_{ij}} \\ \dfrac{\partial^2 \Pi}{\partial s_{ij} \partial r_{ij}} & \dfrac{\partial^2 \Pi}{\partial s_{ij} \partial t_{ij}} & \dfrac{\partial^2 \Pi}{\partial {s_{ij}}^2} \end{bmatrix} \tag{9}$$

3. The Performance Function of a Bistable Laminate

We now define the Limit State Function (LSF) that will be used in our analysis of the bistability probability of bistable composite laminates. For this purpose, the uncertain material properties, laminate dimensions and environmental conditions are considered as random variables; the probability distribution of these random variables is assumed to be normal based on goodness-of-fit test results [31–33]. The total potential energy then becomes a function of the generalized coordinates X and the input parameters, as

$$\Pi = \Pi(X, E_{11}, E_{22}, \upsilon_{12}, G_{12}, \alpha_{11}, \alpha_{22}, \beta_{22}, \Delta T, \Delta C, L_x, L_y, t_{ply})$$

The limit state function (LSF) is defined as

$$g = J_{ij} = \frac{\partial^2 \Pi}{\partial X_i \partial X_j} \tag{10}$$

The limit state function in Eq. (10) is such that $g \leq 0$ defines the unstable configuration (or failure) while $g > 0$ is the stable configuration (or safe). This assumes that bistable behavior is not required; a similar formulation for applications that require a bistable structure would define failure as a mono-stable structure (i.e. the negative of Eq. (10)). Reliability analysis methods are now used to approximate the failure probability; such methods are most efficient when this failure probability is small, as would be expected for an optimum structure that is robust with respect to parameter uncertainties. In this paper, the SS method is applied to estimate the failure probability, since SS is a more efficient and robust algorithm for reliability problems with small failure probability. The details of the SS algorithm are now summarized.

4.1. Subset Simulation of Failure Probability

Reliability analysis evaluates the failure probability of complex engineering systems due to the uncertainty associated with the input quantities. For this purpose, two major groups of methods are available to estimate the failure probability, namely simulation (Monte Carlo Simulation (MCS), Subset Simulation (SS) [34–36], Important Sampling (IS) [37,38], Line Sampling (LS)

[39,40] and so on) and analytical methods (First Order Method (FORM), Second Order Method (SORM)). The aim of these methods is to approximate the integral

$$P_f = \int I_F(\boldsymbol{x}) f(\boldsymbol{x}) \boldsymbol{dx} \tag{11}$$

where $\boldsymbol{x}$ is a vector of uncertain parameters with probability density function (PDF) $f(\boldsymbol{x})$. $I_F(\boldsymbol{x})$ is an indicator function with $I_F(\boldsymbol{x}) = 1$ when $\boldsymbol{x} \in F$ and $I_F(\boldsymbol{x}) = 0$ otherwise, where F is the failure domain. MCS is a robust method to estimate accurate failure probability for any reliability problem but has a substantial computational cost for complex problems with small probabilities [41]. To reduce the cost, various simulation methods have been developed. For instance, SS is more efficient simulation approach to estimate small failure probabilities, for example $P_f < 10^{-3}$. This method was proposed by Au and Beck [36] and has since been further developed to achieve more accuracy and efficiency. In SS, a failure event is converted into a sequence of failure events as $F_1 \supset F_2 \supset ... \supset F_m = F$, where the failure event is defined as $F = \{\boldsymbol{x}: g(\boldsymbol{x}) < 0\}$, and $g(\boldsymbol{x})$ is the LSF. The sequence of failure events is defined here as $F_k = \{\boldsymbol{x}: g(\boldsymbol{x}) < b_k\}$, $(k = 1,2,..,m)$, so that $F_k = \bigcap_{i=1}^{k} F_i$. A set of failure events with thresholds (b_k) are shown schematically in Fig. 1. By using the conditional probability, SS estimates the failure probability as

$$\begin{aligned} P_f = P(F_m) = P\left(\bigcap_{k=1}^{m} F_k\right) \\ = P\left(F_m \middle| \bigcap_{k=1}^{m-1} F_k\right) P\left(\bigcap_{k=1}^{m-1} F_k\right) = \ldots \end{aligned} \tag{12}$$

$$= P(F_1)\prod_{k=1}^{m-1} P(F_{k+1}|F_k)$$

where $P(F_{k+1}|F_k)$ is the conditional probability and the SS failure probability P_f is smaller than the conditional probability. It should be noted $P(F_{k+1}|F_k)$ is typically in the range (0.1-0.3) [42]. The thresholds (b_k) are selected as $N \times P_0$ sorted responses of the system $g(\boldsymbol{x})$ in ascending order $b_k = g(\boldsymbol{x}_{[P_0N]})$. It should be mentioned N is the sample size in each subset and P_0 is the conditional probability.

In Eq. (12), P_1 may be estimated by MCS as

$$P_1 = \frac{1}{N}\sum_{i=1}^{N} I_{F_1}(\boldsymbol{x}_i^{(1)}) \tag{13}$$

where $\boldsymbol{x}_i^{(1)}$ are identical and independent distributed (i.i.d.) samples which are provided by the PDF, $f(\boldsymbol{x})$. The efficiency of SS depends on choosing a suitable sampling technique. Markov Chain Monte Carlo (MCMC) is powerful procedure to produce the conditional samples for the intermediate subsets. To generate samples for the next subset requires the selection of $N \times P_0$ samples as seeds $\{x_1, x_2, ..., x_{[NP_0]}\}$. The new sample in each subset is generated based on the seeds which play an important role in SS [43]. The last conditional probability is estimated as

$$P\left(F_m \middle| F_{m-1}\right) \approx P_m = \frac{1}{N}\sum_{i=1}^{N} I_{F_m}(g(\boldsymbol{x}_i)) = \frac{N_f}{N} \tag{14}$$

Finally, the SS failure probability based on Eqs. (12), (13) and (14) is given by

$$P_f = \prod_{k=1}^{m} P_k \tag{15}$$

4.2. Subset Simulation Sensitivity Analysis

The main aim of sensitivity analysis is to determine the rate of change in the failure probability due to statistical properties of the random variables [44,45]. This gives important information about how to increase or decrease the failure probability by varying the statistical properties of the random parameters. The sensitivity analysis is defined using the partial derivatives of P_f with respect to the distribution parameters ξ (i.e. the mean, μ_{x_i}, or standard deviation, σ_{x_i}) of the random parameters. Thus,

$$\frac{\partial P_f}{\partial \xi} = \sum_{i=1}^{m} \frac{P_f \partial P_i}{P_i \, \partial \xi} \tag{16}$$

Based on Eq .(16), the sensitivity analysis with respect to ξ can be expressed as:

$$\frac{\partial P_f}{\partial \xi_{x_j}} = \frac{P_f \, \partial P_{F_1}}{P_{F_1} \partial \xi_{x_j}} + \sum_{i=2}^{m} \frac{P_{F_1}}{P(F_i|F_{i-1})} \frac{P(F_i|F_{i-1})}{\partial \xi_{x_j}}, j = 1,2,\ldots,N \tag{17}$$

The first and second term are given explicitly as

$$\frac{\partial P_f}{\partial \xi_{x_j}} = \frac{1}{N} \sum_{k=1}^{N} \left(\frac{I_{F_1}(\boldsymbol{x}^k)}{f(\boldsymbol{x}^k)} \frac{\partial f(\boldsymbol{x}^k)}{\partial \xi_{x_j}} \right) \tag{18}$$

$$\frac{P(F_i|F_{i-1})}{\partial \xi_{x_j}} = \frac{1}{N} \sum_{k=1}^{N} \left\{ I_{F_i}(\boldsymbol{x}^k) \left[\frac{1}{\partial f(\boldsymbol{x}^k)} \frac{\partial f(\boldsymbol{x}^k)}{\partial \xi_{x_j}} - \sum_{l=1}^{i-1} \frac{1}{P(F_l|F_{l-1})} \frac{\partial P(F_l|F_{l-1})}{\partial \xi_{x_j}} \right] \right\} \tag{19}$$

By substituting Eqs. (18) and (19) into Eq. (17), the partial derivative of the failure probability with respect to the distribution parameters ξ can be estimated.

5. Example Results

Examples of flat plates are now considered, where bistability is considered as a failure of the manufacturing process. The four baseline bistable composite plates are made of Graphite/Epoxy (T300/5208) with unsymmetric stacking sequences [0/90], [-15/75], [-30/60] and [-45/45] and 150 mm ×150 mm side length. The mean and the coefficient of variation (COV) of the geometry and material properties are listed in Table 1. The coefficient of moisture expansion in the fiber direction (β_{11}) is very small and hence assumed to be zero. It is assumed that the material properties and the fiber distribution in each lamina are uniform. In addition, material properties are assumed to be independent of temperature. Furthermore, the room and cure temperature are considered as 25℃ and 165℃, respectively.

In this work twelve random variables are considered. The bistability probability is calculated using the approach proposed in this paper and summarized in Fig. 2.

5.1. Characteristics of Stable States

Before studying the effect of uncertainties in the parameters, we first determine the stable static configurations. These states for the square cross-ply and angle-ply bistable laminates are obtained by solving Eq. (9), and the results are shown in Fig. 3. At room temperature there are two cylindrical stable states for the cross-ply bistable composite laminates, which have curvature in perpendicular directions. For angle-ply laminates, the shapes are not exactly cylindrical, with a twisted state in addition to the cylindrical shape to give twisted cylindrical or paraboloid configurations. In this figure the analytical results are represented by the continuous surfaces and the FE results are shown by black dots. In the case of bistable composite laminates the accuracy of the analytical method is compared to FEM using the values of the corner displacement.

To validate the analytical model, the maximum transverse displacement of the plates is calculated and presented in Table 2. The results of the analytical method are compared to the results from a finite element analysis. ABAQUS is employed to investigate the bistable composite plate response by the finite element method; the plate is meshed with the S4R elements, and the model consists of 2500 elements and 2061 nodes. Because of the geometrical nonlinearity in these laminates, the 'Static, General' step considering geometric nonlinearity 'Nlgeom' is employed for the static analysis. To simulate the stable states an initial imperfection should be imposed on the laminates, since all of the laminates considered in this manuscript are square. Hence, two 'static general' steps should be defined, where in the first step the initial imperfections given as four tiny forces are applied at the corners of laminates, and then in the second step these imperfections are removed. These results show that analytical method has an acceptable accuracy (about 2% error).

The region of parameter space that gives bistability depends on the length and thickness of the plate, and hence for a specific range of the plate dimensions there are two stable states. The critical geometrical dimensions are determined by the analytical method for a square plate and are listed in Table 3. For example, Table 3 shows that there is only one stable state for the [0/90] bistable plate if the length is less than 54.37mm or the thickness be more than 2.02mm. By determining the change in the curvature with respect to the side length the critical point (bifurcation point) can move toward smaller lengths, and the range of bistability will increase. Figure 4 shows a typical example of the curvature as the length changes, showing the bifurcation to a bistable plate.

The material properties, ambient temperature and moisture have a significant impact on whether a plate is bistable and on the bistability characteristics. Considering the impact of the moisture is critical due to the wide range of applications of bistable composite laminates in aerospace structures. Moisture absorption from the environment by composite materials can be substantial which leads to changes in the stress field and influences the bistable characteristics. By considering 0.6 wt% moisture content, which is approximately the maximum moisture content a laminate could absorb [46], the critical length is equal to 92.26 mm, which highlights that the bistability region decreases dramatically. Consequently, recognizing and investigating the effects of these factors on bistability is very important. In next section, the effect of these uncertainty sources on the bistability probability will be investigated.

5.2. Reliability Analysis

The reliability analysis is now used to predict the effect of the design parameters on bistable behavior of composite plates. The bistability probability of five bistable laminates are estimated by the SS approach. This approach only requires a small number of evaluations of the LSF, and is more efficient for complex structures for the calculation of a high reliability index, compared to MCS. It should be mentioned that the conditional probability is considered as $P_0 = 0.1$. Tables 4 and 5 show the bistability probability of different laminates both without moisture effects and with moisture (0.6 wt%) effects for the statistical properties given in Table 1. According to these tables, the bistability probability for the [0/90] and [-30/60] laminates are the highest and the bistability probability achieved are 0.0139 and 0.0118 respectively. In other words, the probability of a cross-ply laminate being bistable is higher than for an angle-ply laminate. In addition, the moisture absorption decreases the bistability probability in the cross-ply laminate. The SS results are close to the reference values obtained by MCS but also require fewer LSF evaluations. In addition to the comparison of the SS results to MCS analysis, the number of subsets is investigated to avoid getting trapped in misleading situations. In detail, when the number of subsets is small (in this paper, less than 6) and convergence has occurred due to samples falling in the favorable/correct failure region, the problem is not categorized as "misleading", and SS provides reliable results. A detailed discussion on the problem of misleading functions and how to address these problems can be found on [34]. In the final step, the influence of each variable on the bistable region is now investigated.

5.3. Sensitivity Analysis

The objective of this work is to extract the sensitivity of the bistable response of the composite laminates with respect to the parameters that describe the distribution of the geometrical descriptors, material properties, ambient temperature and humidity. Based on Eqs. (17)-(19), the sensitivity of the bistability probability is shown in Fig. 5. The reliability sensitivity results in Fig. 5(a) show that the mean values of the parameters α_{22}, E_{22} and G_{12} have a positive influence on reliability, i.e. the reliability improves with an increase in the mean values of these parameters, since the bistability probability reduces**.** However, the reliability reduces with an increase in the mean values of β_{22}, ΔM, t_{ply}, T_{room}, α_{11}, E_{11} and υ_{12}. The mean value of parameter α_{22} has the highest effect on the increasing bistability probability. On the other hand, β_{22} , ΔM and t_{ply} have the highest impact on increasing the bistability probability. Other variables (G_{12}, E_{11}, E_{22}, υ_{12}) have insignificant effects. It is observed from Fig. 5(b) that the standard deviations have the same effects as the mean values on the probability bistability, although of course the levels vary. This analysis gives the effect of the parameters on the bistable behavior, although the design engineer would also need to consider the associated cost to decrease or increase the mean and/or standard deviation of specific parameters.

The sensitivity analysis illustrates that uncertainty in the thermal and moisture expansion coefficients, temperature, humidity and thickness have substantial influences on the region of bistability. In the following, the sensitivity of the bistable region to ±10% changes in these parameters for a [0/90] bistable laminate, including the moisture level, are determined using the analytical method and are listed in Table 6. Thus a +10% variation in α_{22}, decreases the critical length by 13.31% which means that the bistability region enlarges. However, a +10% variation in the other parameters, shrinks the bistability region and the effect of b_{22} is higher than the others.

The results for the [0/90] bistable plate without moisture effects is given in Table 7. Here the thickness of the laminate has the most influence on the bistable behaviour, and +10% increase leads to a 9.91% decrease in the critical length at the bifurcation point.

6. Conclusions

The increasing use of composites in engineering structures means that studying the effect of the design variables on the bistable characteristics is essential. This paper has estimated and analyzed the bistability probability for [0/90], [-15/75], [-30/60] and [-45/45] lay-ups composite laminates using the subset simulation method. The results show that the [0/90] and [-30/60] laminates have a higher probability to behave as bistable composites. Furthermore, moisture absorption leads to a reduction in the probability that the laminate will be bistable. The sensitivity analysis has shown that the transverse coefficient of thermal expansion increases the bistability probability. But, coefficient of moisture, moisture content, thickness, longitudinal coefficient of thermal expansion and room temperature reduce the probability. Other parameters ($E_{11}, E_{22}, \upsilon_{12}, G_{12}$) have an insignificant effect on the bistability region. In order to validate results, those obtained from the SS method were compared with Monte Carlo simulation and those determined by the analytical method were verified by FEM. This approach can be used for complex and multistable composite structures.

Data Availability

This paper does not use any raw data. The results may be obtained by following the analysis approach described using the data given in the tables.

Reference

[1] Daynes S, Weaver PM, Trevarthen JA. A morphing composite air inlet with multiple stable shapes. J Intell Mater Syst Struct 2011;22:961–73.

[2] Bilgen O, Arrieta AF, Friswell MI, Hagedorn P. Dynamic control of a bistable wing under aerodynamic loading. Smart Mater Struct 2013;22:25020.

[3] Arrieta AF, Bilgen O, Friswell MI, Ermanni P. Modelling and configuration control of wing-shaped bi-stable piezoelectric composites under aerodynamic loads. Aerosp Sci Technol 2013;29:453–61.

[4] Kuder IK, Fasel U, Ermanni P, Arrieta AF. Concurrent design of a morphing aerofoil with variable stiffness bi-stable laminates. Smart Mater Struct 2016;25:115001.

[5] Nicassio F, Scarselli G, Pinto F, Ciampa F, Iervolino O, Meo M. Low energy actuation technique of bistable composites for aircraft morphing. Aerosp Sci Technol 2018;75:35–

46.

[6] Zhang Z, Li X, Yu X, Chai H, Li Y, Wu H, et al. Magnetic actuation bionic robotic gripper with bistable morphing structure. Compos Struct 2019;229:111422.

[7] Zhang Z, Chen B, Lu C, Wu H, Wu H, Jiang S, et al. A novel thermo-mechanical anti-icing/de-icing system using bi-stable laminate composite structures with superhydrophobic surface. Compos Struct 2017;180:933–43.

[8] Zhang Z, Pei K, Sun M, Wu H, Yu X, Wu H, et al. A novel solar tracking model integrated with bistable composite structures and bimetallic strips. Compos Struct 2020;248:112506.

[9] Pan D, Dai F. Design and analysis of a broadband vibratory energy harvester using bi-stable piezoelectric composite laminate. Energy Convers Manag 2018;169:149–60.

[10] Saberi S, Ghayour M, Mirdamadi HR, Ghamami M. Free vibration analysis and mode management of bistable composite laminates using deep learning. Arch Appl Mech 2021. https://doi.org/10.1007/s00419-021-01930-4.

[11] Alazwari MA, Rao SS. Modeling and analysis of composite laminates in the presence of uncertainties. Compos Part B Eng 2019;161:107–20.

[12] Saberi S, Abdollahi A, Inam F. Reliability analysis of bistable composite laminates. AIMS Mater Sci 2021;8:29–41.

[13] Hyer MW. Some observations on the cured shape of thin unsymmetric laminates. J Compos Mater 1981;15:175–94.

[14] Hyer MW. The room-temperature shapes of four-layer unsymmetric cross-ply laminates. J Compos Mater 1982;16:318–40.

[15] Akira H, Hyer MW. Non-linear temperature-curvature relationships for unsymmetric graphite-epoxy laminates. Int J Solids Struct 1987;23:919–35.

[16] Ren L, Parvizi-Majidi A, Li Z. Cured shape of cross-ply composite thin shells. J Compos Mater 2003;37:1801–20.

[17] Betts DN, Salo AIT, Bowen CR, Kim HA. Characterisation and modelling of the cured shapes of arbitrary layup bistable composite laminates. Compos Struct 2010;92:1694–700.

[18] Giddings PF, Bowen CR, Salo AIT, Kim HA, Ive A. Bistable composite laminates: effects of laminate composition on cured shape and response to thermal load. Compos Struct 2010;92:2220–5.

[19] Tawfik SA, Dancila DS, Armanios E. Planform effects upon the bistable response of cross-ply composite shells. Compos Part A Appl Sci Manuf 2011;42:825–33.

[20] Pirrera A, Avitabile D, Weaver PM. On the thermally induced bistability of composite cylindrical shells for morphing structures. Int J Solids Struct 2012;49:685–700.

[21] Mattioni F, Weaver PM, Friswell MI. Multistable composite plates with piecewise variation of lay-up in the planform. Int J Solids Struct 2009;46:151–64.

[22] Moore M, Ziaei-Rad S, Salehi H. Thermal response and stability characteristics of bistable composite laminates by considering temperature dependent material properties and resin layers. Appl Compos Mater 2013;20:87–106.

[23] Zhang Z, Ye G, Wu H, Wu H, Chen D, Chai G. Thermal effect and active control on bistable behaviour of anti-symmetric composite shells with temperature-dependent properties. Compos Struct 2015;124:263–71.

[24] Zhang Z, Wu H, Ye G, Yang J, Kitipornchai S, Chai G. Experimental study on bistable behaviour of anti-symmetric laminated cylindrical shells in thermal environments. Compos Struct 2016;144:24–32.

[25] Fujioka E, Yokozeki T, Watanabe A, Aoki T. Analysis on temperature-dependent deployment behavior of bi-stable composite rods. Adv Compos Mater 2019;28:245–57.

[26] Che L, Fang G, Wu Z, Ma Y, Zhang J, Zhou Z. Investigation of curing deformation behavior of curved fiber metal laminates. Compos Struct 2020;232:111570.

[27] Etches J, Potter K, Weaver P, Bond I. Environmental effects on thermally induced multistability in unsymmetric composite laminates. Compos Part A Appl Sci Manuf 2009;40:1240–7.

[28] Zhang Z, Pan H, Wu H, Jiang S, Chai G. Hygroscopic influence on bistable characteristics of antisymmetric composite cylindrical shells: An experimental study. J Compos Mater 2018;52:3565–77.

[29] Wu Y, Gao K, Ren Q. Hydrothermal effect on Bi-stability of composite cylindrical shell. Compos Struct 2020;232:111554.

[30] Brampton CJ, Betts DN, Bowen CR, Kim HA. Sensitivity of bistable laminates to uncertainties in material properties, geometry and environmental conditions. Compos Struct 2013;102:276–86.

[31] Li X, Lv Z, Qiu Z. A novel univariate method for mixed reliability evaluation of composite laminate with random and interval parameters. Compos Struct 2018;203:153–63.

[32] Shaw A, Sriramula S, Gosling PD, Chryssanthopoulos MK. A critical reliability evaluation

of fibre reinforced composite materials based on probabilistic micro and macro-mechanical analysis. Compos Part B Eng 2010;41:446–53.

[33] Jeong HK, Shenoi RA. Probabilistic strength analysis of rectangular FRP plates using Monte Carlo simulation. Comput Struct 2000;76:219–35.

[34] Abdollahi A, Moghaddam MA, Monfared SAH, Rashki M, Li Y. A refined subset simulation for the reliability analysis using the subset control variate. Struct Saf 2020;87:102002.

[35] Au S-K, Beck JL. Estimation of small failure probabilities in high dimensions by subset simulation. Probabilistic Eng Mech 2001;16:263–77. https://doi.org/10.1016/S0266-8920(01)00019-4.

[36] Au SK, Beck JL. Subset Simulation--A New Approach to Calculating Small Failure Probabilities. Proc. Int. Conf. Monte Carlo Simul., 2000, p. 287–93.

[37] Au S-K, Beck JL. A new adaptive importance sampling scheme for reliability calculations. Struct Saf 1999;21:135–58.

[38] Melchers RE. Importance sampling in structural systems. Struct Saf 1989;6:3–10.

[39] Lu Z, Song S, Yue Z, Wang J. Reliability sensitivity method by line sampling. Struct Saf 2008;30:517–32.

[40] Pradlwarter HJ, Schueller GI, Koutsourelakis PS, Charmpis DC. Application of line sampling simulation method to reliability benchmark problems. Struct Saf 2007;29:208–21.

[41] García-Macías E, Castro-Triguero R, Friswell MI, Sáez-Pérez A, Gallego R. Uncertainty analysis of mechanical behavior of functionally graded carbon nanotube composite

materials. Model Valid. Uncertain. Quantif. Vol. 3, Springer; 2016, p. 59–72.

[42] Li H-S, Cao Z-J. Matlab codes of Subset Simulation for reliability analysis and structural optimization. Struct Multidiscip Optim 2016;54:391–410. https://doi.org/10.1007/s00158-016-1414-5.

[43] Abdollahi A, Moghaddam MA, Monfared SAH, Rashki M, Li Y. Subset simulation method including fitness-based seed selection for reliability analysis. Eng Comput n.d.:1–17.

[44] MiarNaeimi F, Azizyan G, Rashki M. Reliability sensitivity analysis method based on subset simulation hybrid techniques. Appl Math Model 2019.

[45] Song S, Lu Z, Qiao H. Subset simulation for structural reliability sensitivity analysis. Reliab Eng Syst Saf 2009;94:658–65. https://doi.org/10.1016/j.ress.2008.07.006.

[46] Portela P, Camanho P, Weaver P, Bond I. Analysis of morphing, multi stable structures actuated by piezoelectric patches. Comput Struct 2008;86:347–56.

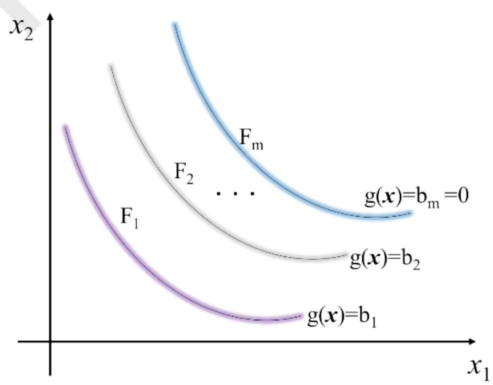

Fig.1 Set of SS failure events in a 2D problem

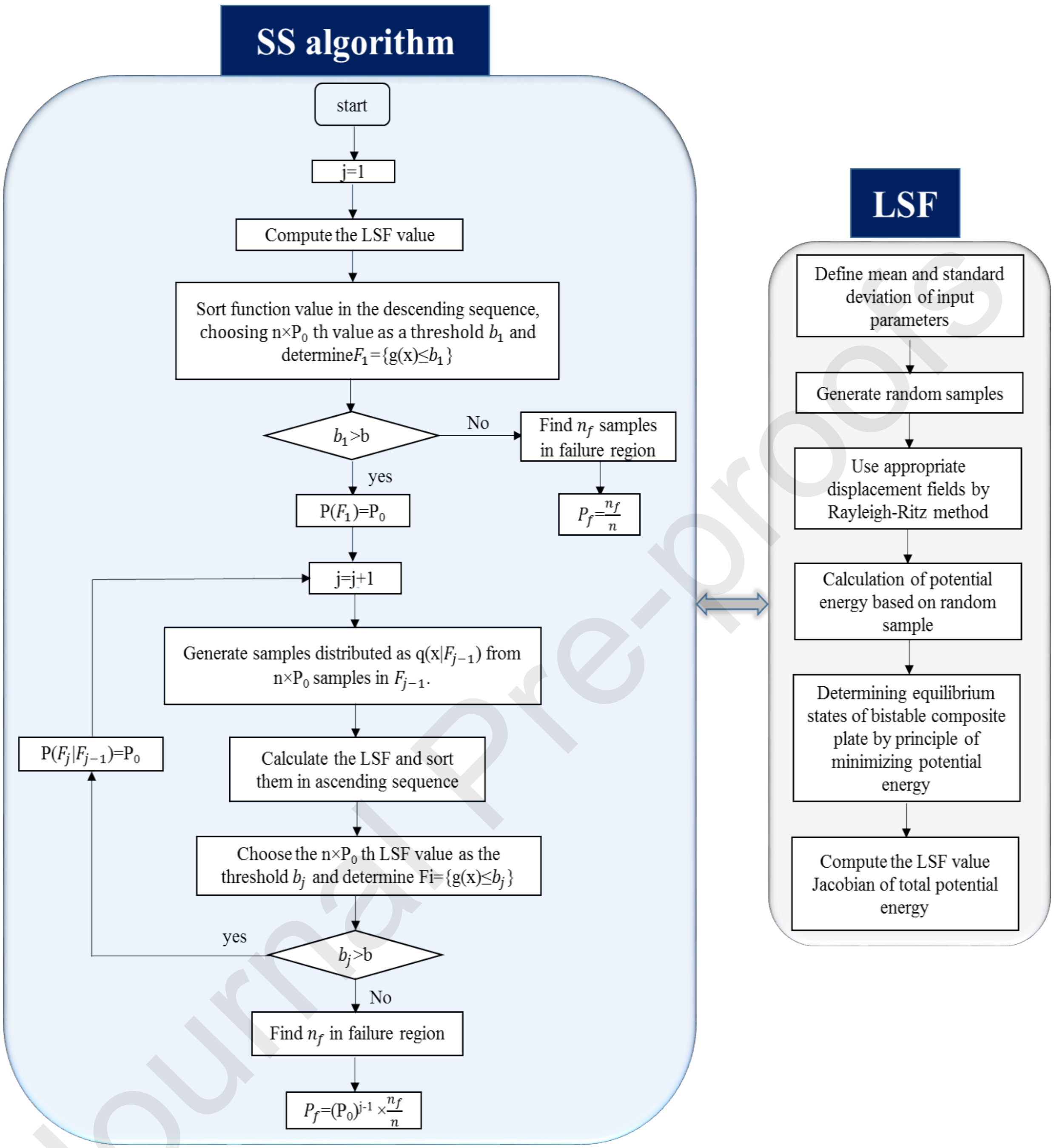

Fig. 2 Flow chart of estimation of the bistability probability by the SS method.

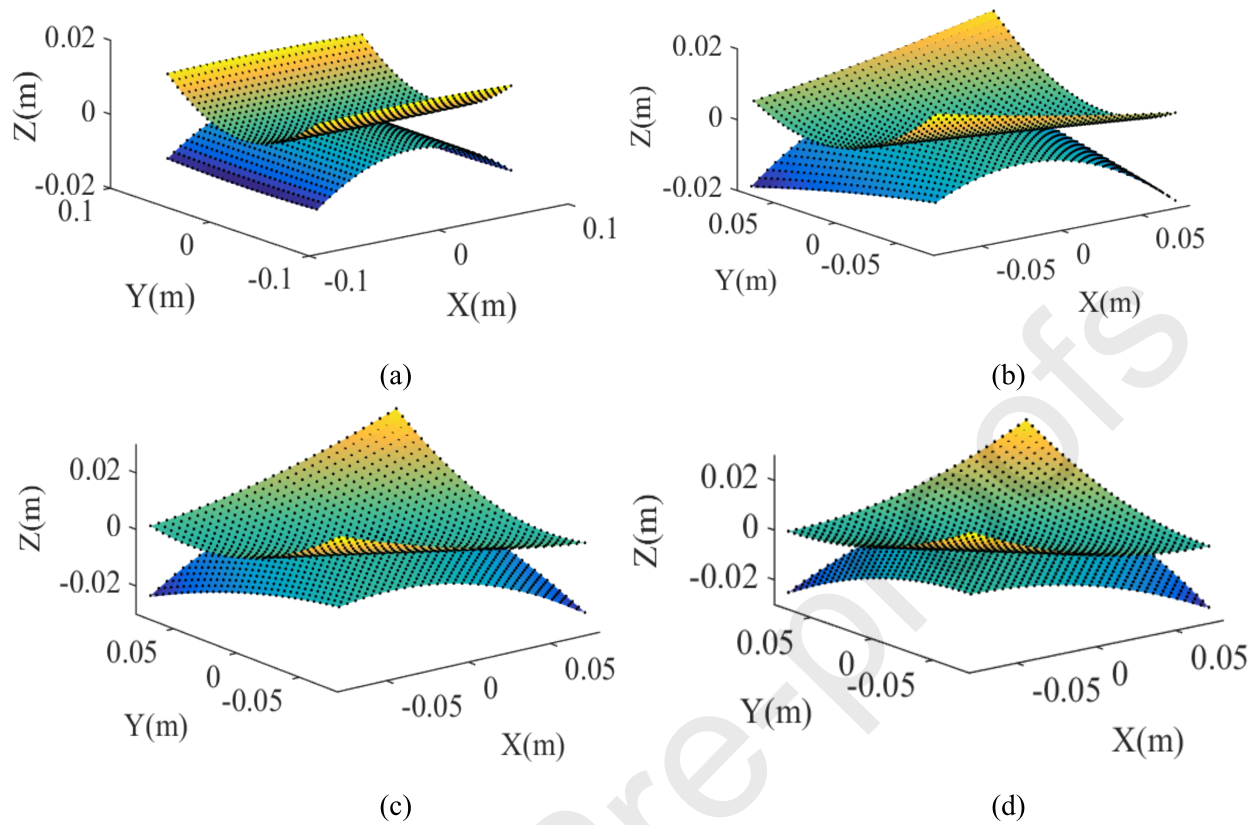

Fig. 3 Stable configurations of the four square bistable composite laminates with different layups: Analytical results are represented by the continuous surfaces and FE results are shown by black dots (a) [0/90] (b) [-15/75] (c) [-30/60] (d) [-45/45]

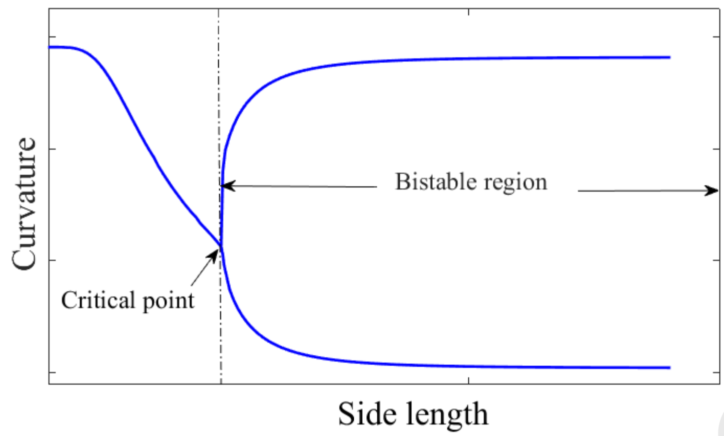

Fig. 4 Varation of the curvature with respect to the side length and the bistable region for a [0/90] bistable composite plate.

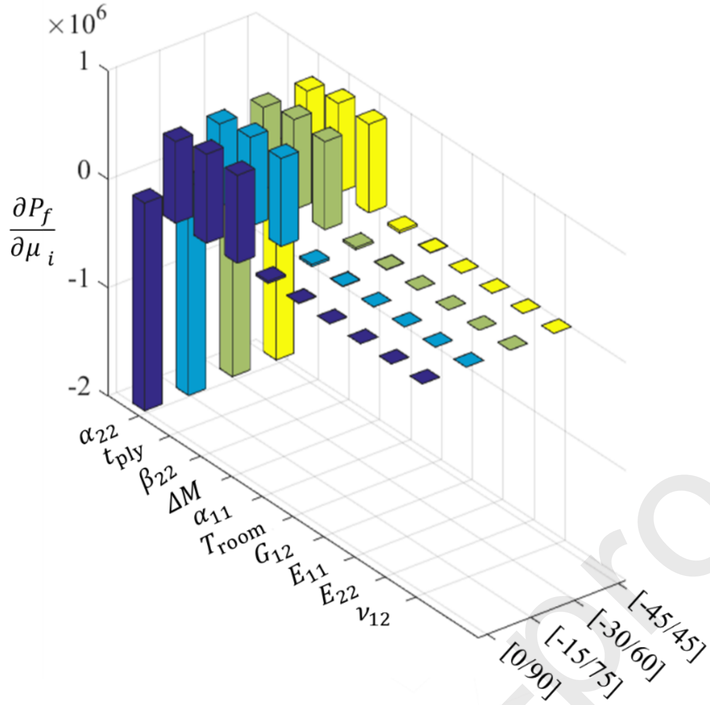

(a)

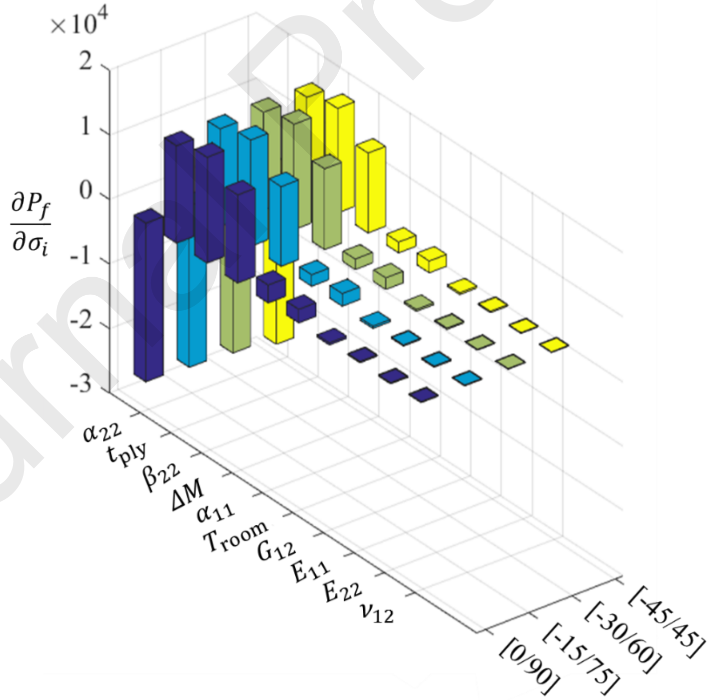

(b)

Fig. 5 Probability sensitivity for four bistable composite laminates with respect to the statistical distribution of the parameters (a) mean (b) standard deviation

Table 1. Statistical properties of the random parameters

RV Index	Property	Mean value	Standard deviation	Distribution type
1	E_{11} [GPa]	146.95	14.695	Normal
2	E_{22} [GPa]	10.702	1.0702	Normal
3	G_{12} [GPa]	6.977	0.6977	Normal
4	ν_{12}	0.3	0.03	Normal
5	$\alpha_{11}[1/℃]$	5.028×10^{-7}	5.028×10^{-8}	Normal
6	$\alpha_{22}[1/℃]$	2.65×10^{-5}	2.65×10^{-6}	Normal
7	$\beta_{22}[1/\text{wt\%}]$	0.005	0.0005	Normal
8	$\Delta M[\text{wt\%}]$	0.6	0.06	Normal
9	$T_{room}[℃]$	25	2.5	Normal
10	t_{ply}[mm]	0.365	0.0365	Normal
11	L_x[mm]	0.150	0.015	Normal
12	L_y[mm]	0.150	0.015	Normal

Table 2. Maximum out-of-plane displacement (mm) at a corner of the [0/90] bistable plate

Type of laminate	FE	Analytical
[0/90]	11.34	11.56

Table 3. Critical dimensions for various lay-ups of the bistable composite laminates.

Type of laminate	Critical length (mm)	Critical thickness (mm)
[0/90]	54.37	2.02
[-15/75]	53.40	2.04
[-30/60]	77.30	1.45
[-45/45]	80.59	1.77

Table 4. The reliability analysis results for different bistable laminates without moisture.

Type of laminate	bistability probability (P_f)-SS	bistability probability (P_f)-MCS	#Evaluation LSF-SS	#Evaluation LSF-MCS
[0/90]	1.39e-2	1.33e-2	6e2	10e4
[-15/75]	0.91e-2	0.87e-2	10e2	10e6
[-30/60]	1.18e-2	1.15e-2	6e2	10e4
[-45/45]	0.96e-2	0.98e-2	10e2	10e6

Table 5. The reliability analysis results for different bistable laminates under moisture (0.6 wt%).

Type of laminate	bistability probability (P_f)-SS	bistability probability (P_f)-MCS	#Evaluation LSF-SS	#Evaluation LSF-MCS
[0/90]	7.38e-3	7.31e-3	15e2	10e4
[-15/75]	2.07e-05	1.19e-05	50e2	10e6
[-30/60]	4.92e-3	4.73e-3	15e2	10e4
[-45/45]	7.930e-04	8.106e-04	40e2	10e6

Table 6. Change of critical length for a ±10% change in the parameters for [0/90] bistable laminate with moisture (0.6 wt%)

Parameter	Percentage change of critical length for ±10% change in each parameter	
	-10%	+10%
β_{22}	-9.32	+9.71
ΔM	-8.91	+9.43
thickness	-15.56	+8.64
α_{22}	+17.08	-13.31
α_{11}	-1.34	+1.09
T_{room}	-3.59	+0.95

Table 7. Change of critical length for a ±10% change in the parameters for a [0/90] bistable laminate

Parameter	Percentage change of critical length for ±10% change in each parameter	
	-10%	+10%
thickness	-9.91	+9.91
α_{22}	+5.49	-4.72
α_{11}	-0.57	+0.51
T_{room}	-1.83	+0.36

Author Contributions

Saeid Saberi: Conceptualization, Methodology, Writing - Original draft preparation,

Azam Abdollahi: Software, Investigation, Writing - Review & Editing

Michael I Friswell: Supervision, Writing - Review & Editing